

000  
001  
002  
003  
004  
005  
006  
007  
008  
009  
010  
011  
012  
013  
014  
015  
016  
017  
018  
019  
020  
021  
022  
023  
024  
025  
026  
027  
028  
029  
030  
031  
032  
033  
034  
035  
036  
037  
038  
039  
040  
041  
042  
043  
044  
045  
046  
047  
048  
049  
050  
051  
052  
053  

# ANY-ORDER ANY-SUBSET AUTOREGRESSIVE MODEL

**Anonymous authors**

Paper under double-blind review

## ABSTRACT

We propose Any-order Any-subset Autoregressive modeling (A3), a novel sequence generation framework that generalizes standard autoregressive (AR) factorization to support the prediction of arbitrary token groups in any order. A3 overcomes the limitations of conventional left-to-right decoding by enabling flexible groupwise generation while preserving probabilistic rigor and training stability. Our design combines a two-stream attention architecture with a progressive training strategy, allowing both efficient parallel decoding and robust modeling of diverse dependency structures. Empirical results demonstrate that A3 achieves a superior trade-off between generation speed, flexibility, and quality compared to state-of-the-art AR and diffusion-based methods. This work offers a unified approach for a flexible, efficient, and novel language modeling paradigm.

## 1 INTRODUCTION

Autoregressive (AR) modeling has been the dominant paradigm for text generation, underpinning the success of most large language models (Touvron et al., 2023; Bai et al., 2023a; Radford et al., 2018). In the AR framework, the joint probability of a token sequence is factorized in a fixed left-to-right order, generating one token at a time. While simple and effective, this formulation imposes several intrinsic limitations. For example, the strict left-to-right ordering prevents models from fully exploiting bidirectional context during generation. Also, the one-token-at-a-time decoding process creates a computational bottleneck that limits generation efficiency. These fundamental drawbacks constrain both modeling flexibility and decoding speed, especially in long-context and complex generation scenarios (Kuratov et al., 2024; Bai et al., 2023b).

Alternative approaches such as masked diffusion language models (Li et al., 2022; Gong et al., 2025; Gulrajani & Hashimoto, 2024) attempt to address these limitations by enabling parallel prediction of multiple tokens. By iteratively denoising partially masked sequences, diffusion models can achieve any-order generation and leverage bidirectional context. However, these methods introduce new challenges: they often require carefully tuned noise schedules and multi-step inference, which complicates training and slows decoding, and they typically yield less stable training dynamics and lower sample quality compared to AR approaches (Kim et al., 2025).

In this work, we propose **Any-order Any-subset Autoregressive modeling** (A3), a new framework that merges the strengths of AR modeling with the flexibility of parallel generation. A3 generalizes the standard AR factorization by partitioning the sequence into arbitrary groups of tokens and predicting them in any order. This groupwise factorization retains the probabilistic rigor of AR models while enabling flexible dependency structures, bidirectional conditioning, and efficient groupwise decoding.

To realize A3 in practice, we design a two-stream attention architecture that supports arbitrary group orderings, and develop a progressive training strategy that adapts pretrained AR models to any-order prediction. Our framework naturally supports diverse inference strategies, including groupwise AR sampling and dynamic resampling, offering a tunable trade-off between generation speed and quality.

Through comprehensive experiments on question answering (Joshi et al., 2017), commonsense reasoning (Zellers et al., 2019; Sakaguchi et al., 2020; Sap et al., 2019; Bisk et al., 2020), and story infilling tasks (Mostafazadeh et al., 2016), we show that A3 achieves strong performance across diverse benchmarks while enabling flexible and efficient generation. Notably, A3 outperforms state-of-the-art diffusion-based models despite using substantially less training data, and demonstrates

054 promising scaling behavior with model size. These results suggest that A3 provides a new direction  
 055 for bridging the gap between AR and parallel generation paradigms.  
 056

057 Our contributions can be summarized as follows:

- 058 • **Conceptually**, we propose A3, a novel language modeling framework that leverages both  
 059 insights from AR modeling and parallel generation. With groupwise token partition, A3  
 060 successfully enables flexible generation at *any subset in any order*.
- 061 • **Practically**, we implement A3 for both training and inference phases. Building on a novel  
 062 attention architecture that supports arbitrary group orderings, A3 can be trained progres-  
 063 sively to adapt pretrained AR models to any-order prediction during inference.
- 064 • **Empirically**, we evaluate A3 across diverse reasoning and QA benchmarks to demonstrate  
 065 its strong performance while enabling flexible and efficient generation, showing its great  
 066 potential serving as next-generation of language modeling paradigm.

## 068 2 ANY-ORDER ANY-SUBSET AUTOREGRESSIVE MODELING

### 069 2.1 FORMULATION

070 In this section, we will demonstrate the formulation of our proposed Any-order Any-subset Autore-  
 071 gressive modeling (A3). The dominant paradigm for text generation is autoregressive (AR) model-  
 072 ing, where the joint probability of a sequence  $x_{1:N}$  with length  $N$  is factorized in a fixed left-to-right  
 073 order:

$$074 P(x_{1:N}) = \prod_{t=1}^N P(x_t | x_{<t}). \quad (1)$$

075 This formulation is simple, effective, and fundamental to most large language models (Touvron  
 076 et al., 2023; Bai et al., 2023a; Radford et al., 2018). However, it introduces two key limitations.  
 077 First, the left-to-right constraint forces the model to generate tokens sequentially, preventing it from  
 078 leveraging bidirectional context during both training and inference. Second, decoding proceeds one  
 079 token at a time, creating a bottleneck of inference efficiency. Together, these limitations restrict the  
 080 model’s ability to fully exploit contextual information and achieve faster generation.

081 Alternative paradigms such as masked diffusion models (Li et al., 2022; Gong et al., 2025; Gulrajani  
 082 & Hashimoto, 2024) attempt to overcome the speed bottleneck by generating multiple tokens in  
 083 parallel. Concretely, the index set  $1, 2, \dots, N$  is partitioned into two disjoint subsets: a unmasked  
 084 index group  $G_1$  and its masked complement  $G_2$ . The model then predicts the masked tokens  $x_{G_2}$   
 085 conditioned on the visible tokens  $x_{G_1}$ :

$$086 P(x_{G_2} | x_{G_1}) = \prod_{t \in G_2} P(x_t | x_{G_1}). \quad (2)$$

087 During inference, the model starts from a fully masked sequence (i.e.,  $G_2 = \emptyset$ ) and iteratively de-  
 088 noises it by resampling subsets of positions, filling in multiple tokens at each step. This procedure  
 089 alleviates the inference-speed limitation of AR models by enabling parallel token generation. How-  
 090 ever, masked diffusion models suffer from two key drawbacks. First, since only a subset of tokens  
 091 is predicted in each training step, the learning signal is partial and less informative, often yielding  
 092 lower sample quality compared to AR models. Second, the training dynamics are unstable: perfor-  
 093 mance depends heavily on carefully tuned noise schedules, masking strategies, and iteration counts,  
 094 which complicates optimization and make it difficult to achieve consistent performance (Kim et al.,  
 095 2025).

096 We now seek a middle ground: a model that preserves the probabilistic rigor of AR modeling while  
 097 enabling flexible prediction orders and parallelism in decoding. This motivates **Any-order Any-**  
 098 **subset Autoregressive** modeling (A3), which extends the AR framework to group-level prediction.  
 099 Instead of using a fixed left-to-right order with unit-sized steps, A3 factorizes the joint probability  
 100 by partitioning the token sequence into groups:

$$101 P(x_{1:N}) = \prod_{k=1}^K P(x_{G_k} | x_{g_{<k}}). \quad (3)$$

108 where  $G_1, G_2, \dots, G_K$  is a partition of the tokens and each group  $G_k$  may contain one or more  
 109 tokens. Crucially, the ordering of groups is arbitrary, which enables flexible dependency structures.  
 110

111 By training the model on random groupings and permutations, we expose it to a wide variety of  
 112 factorization orders, forcing it to learn robust conditional dependencies beyond simple left-to-right  
 113 context. This resembles the permutation LM objective of XLNet (Yang et al., 2019) but at the group  
 114 level, enabling richer structural modeling.

## 116 2.2 DISCUSSION WITH PREVIOUS PARADIGMS

119 **Comparison with Masked Diffusion Language Models.** Masked diffusion language models  
 120 (MDLMs) have recently emerged as an alternative to AR decoding, aiming to overcome the se-  
 121 quential bottleneck of one-token-at-a-time generation. By iteratively denoising partially masked  
 122 sequences, MDLMs can update multiple tokens in parallel and exploit bidirectional context (Austin  
 123 et al., 2021; Li et al., 2022; Gong et al., 2025; Nie et al., 2025). This flexibility enables controllable,  
 124 any-order generation and supports tasks such as infilling and global rewriting. However, diffusion  
 125 approaches face two major limitations. First, inference speed is constrained by the need for many  
 126 iterative refinement steps, with generation efficiency depending critically on noise schedules and  
 127 step counts (Gong et al., 2025). While large-scale efforts such as DiffuGPT and LLaDA demon-  
 128 strate that diffusion LMs can match or surpass AR models in quality, they still require careful tuning  
 129 and incur nontrivial decoding costs (Gong et al., 2025; Nie et al., 2025). Second, training stability  
 130 is less favorable than AR: discrete diffusion objectives require complex forward-reverse processes  
 131 and additional pretraining or adaptation, making optimization more resource-intensive and sensitive  
 132 to hyperparameters (He et al., 2023).

133 In contrast, A3 preserves the probabilistic rigor and training simplicity of AR modeling while in-  
 134 troducing flexible groupwise factorization. This allows parallel prediction of token subsets without  
 135 relying on multi-step denoising schedules, thereby offering both efficiency and stability.

136 **Comparison with AR Multi-Token Prediction.** Another line of work seeks to improve AR effi-  
 137 ciency by enabling the model to predict multiple future tokens per step (Gloeckle et al., 2024; Kou  
 138 et al., 2024). Multi-token objectives and speculative decoding significantly reduce inference latency:  
 139 for instance, predicting four tokens at once can yield up to threefold speedups while preserving or  
 140 even improving generation quality, particularly in reasoning and code generation tasks (Gloeckle  
 141 et al., 2024). These methods retain the training stability of standard AR, since the additional ob-  
 142 jectives can be implemented as auxiliary losses with negligible computational overhead. However,  
 143 multi-token prediction remains bound to a fixed left-to-right ordering, limiting its modeling flexibil-  
 144 ity. The approach accelerates sequential decoding but does not enable infilling, bidirectional con-  
 145 ditioning, or arbitrary ordering of token generation. Moreover, these methods depend on multiple  
 146 linear heads, which limits maximum parallelism. Therefore, they cannot reach the same theoretical  
 147 decoding parallelism as diffusion-style iterative refinement. A3, by contrast, can reuse diffusion-  
 148 like scheduling using a single AR model, enabling it to achieve a higher theoretical upper bound on  
 149 parallel decoding efficiency while remaining within an AR framework.

150 A3 generalizes beyond this paradigm by relaxing the strict AR factorization. Through arbitrary  
 151 group partitions and orderings, A3 supports both sequential and parallel decoding strategies, com-  
 152 bining the efficiency gains of multi-token prediction with greater structural flexibility. For more  
 153 discussions with related work, refer to Appendix B.

## 154 3 IMPLEMENTATIONS OF TRAINING AND FLEXIBLE INFERENCE

155 In this section, we describe the implementation of A3. We begin with the architectural design  
 156 of A3, where we use a two-stream attention mechanism to enable predictions in arbitrary orders.  
 157 Next, we present our efficient continuous pretraining strategy, which progressively adapts the model  
 158 from standard AR prediction to group-based prediction. Finally, we introduce the flexible inference  
 159 strategy of A3, which leverages its general formulation to support diverse decoding modes.

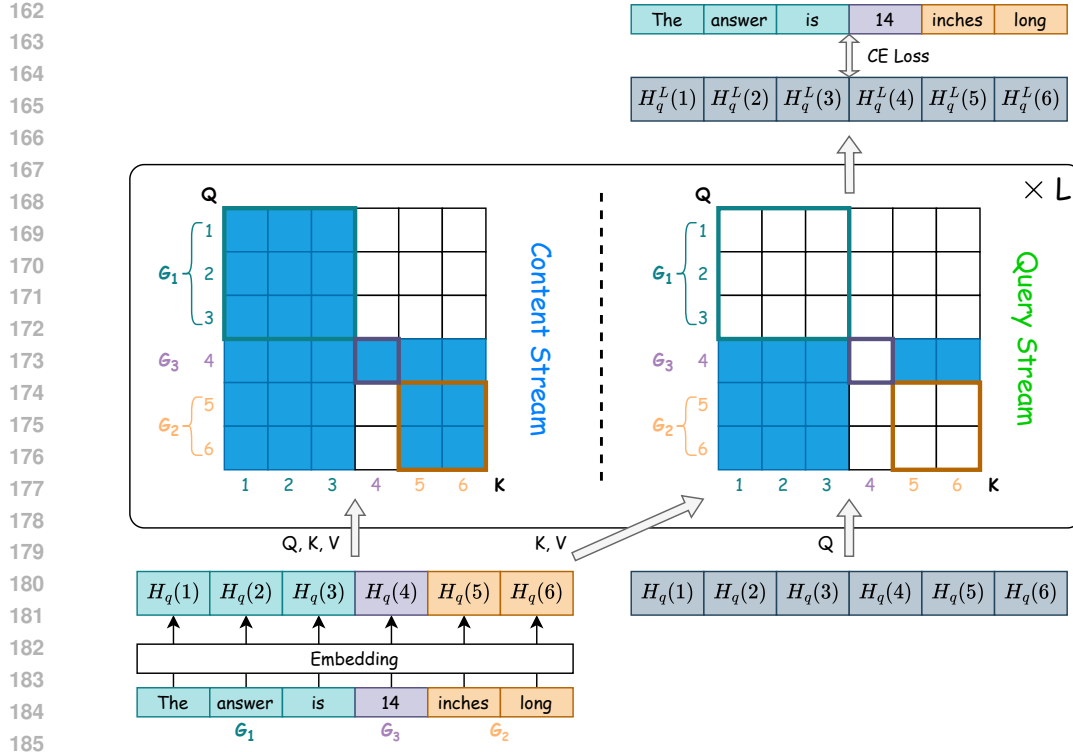


Figure 1: Architecture of the A3 model. Blue entries in the attention mask denote 0, and white entries denote  $-\infty$ . The model employs a two-stream attention module with distinct causal masks. The content stream encodes contextual information and attends to tokens within its own group as well as all preceding groups. The query stream encodes positional conditions and attends only to tokens in preceding groups. The final cross-entropy loss is computed between the input context and the query stream’s output. For illustration, we provide an example grouping with  $G_1 = \{1, 2, 3\}, G_2 = \{5, 6\}, G_3 = \{4\}$ , showing how the forward process and causal masks are applied.

### 3.1 ARCHITECTURE DESIGN WITH TWO-STREAM ATTENTION

**Limitations of Current Architecture.** The decoder-only Transformer has become the backbone of modern large language models due to its simplicity and effectiveness in next-token prediction. It operates with a single stream of hidden states, where information flow is regulated by a causal attention mask. This mask ensures that the representation of the  $k$ -th token can only attend to the first  $k$  tokens, thereby enforcing the AR constraint required for language modeling. While well-suited for the standard left-to-right objective, this design assumes a fixed generation order: given the first  $k$  tokens, the model is trained to treat the  $(k + 1)$ -th position as the unique next target. Such rigidity makes it incompatible with any-order prediction, where the next position to be generated need not follow the sequential index.

The encoder-only Transformer, widely used in masked language modeling, represents the opposite design. Rather than causal masking, it processes the full sequence bidirectionally, with missing information represented by mask tokens. Through position embeddings on these masks, the model identifies which locations are to be predicted, allowing arbitrary subsets of tokens to be reconstructed simultaneously. However, this formulation limits dependency modeling: masked positions are predicted in parallel and conditioned only on observed context in a single pass. Without recursive, multi-layered dependencies across tokens, the encoder-only approach struggles to match the generative fidelity of AR models.

**Two-stream Attention Design for Any-order Prediction.** To combine the flexibility of encoder-style masking with the dependency modeling strength of autoregression, A3 extend the two-stream attention mechanism proposed by XLNet (Yang et al., 2019). The model maintains two parallel representations for each position: a **content stream**, which encodes semantic and contextual in-

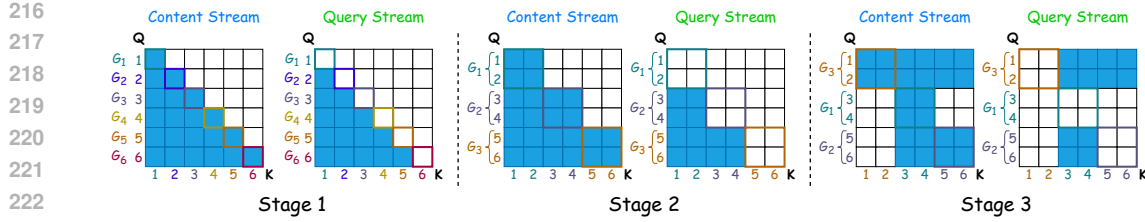


Figure 2: Causal masks for content stream and query stream in different stages. Blue for 0 and white for  $-\infty$ . Stage 1: **AR initialization** to reproduce AR factorization. Stage 2: **Group expansion** by allowing groups of size greater than one. Stage 3: **Order permutation** with introducing any-order prediction.

formation from the observed tokens, and a **query stream**, which provides position-aware signals to drive prediction of the next group. This separation allows A3 to retain the recursive structure of autoregression while relaxing the generation order constraint of decoder-only models. Figure 1 illustrates the pipeline of the forward process.

Formally, let  $X = (x_1, \dots, x_N)$  denote the sequence, partitioned into groups  $\{G_1, \dots, G_K\}$ . In the **content stream**, the input consists of the observed tokens, embedded and passed through Transformer layers with a designed causal mask. This mask ensures that a token at group  $k$  can attend to all tokens in groups  $\leq k$ , i.e., both its own group and all groups before it. Thus, the content stream at group  $k$  aggregates all contextual evidence available up to that point. For group  $G_k$ , the hidden states in the content stream at layer  $l$  are computed as:

$$H_c^{(l)}(i) = \text{Attn}\left(Q = H_c^{(l-1)}(i), K = H_c^{(l-1)}(\leq G_k), V = H_c^{(l-1)}(\leq G_k)\right). \quad (4)$$

In the **query stream**, the input is a shared learnable query vector injected at every position. The key and value matrices are tied to those of the content stream, while the queries are separate. With an appropriately designed causal mask, each query vector at group  $k$  can only attend to content tokens in groups  $< k$ , not including its own group. This forces the query representation to serve as the position-aware predictor for the tokens in group  $k$ , relying only on prior context rather than future information. Conceptually, the query stream specifies *where* to predict (positional conditioning), while the content stream provides *what* to predict (contextual grounding). The hidden states in the query stream at layer  $l$  for group  $G_k$  are:

$$H_q^{(l)}(i) = \text{Attn}\left(Q = H_q^{(l-1)}(i), K = H_c^{(l-1)}(< G_k), V = H_c^{(l-1)}(< G_k)\right), \quad (5)$$

where the initialization  $H_q^{(l-1)}(i) = w$  is a learnable query vector shared across positions, and the causal mask ensures the query stream at group  $k$  can only access content states from strictly earlier groups.

Finally, the predictive distribution for token  $x_i \in G_k$  is parameterized by:

$$p(x_i | X_{< G_k}) = \text{Softmax}\left(W \cdot H_q^{(L)}(i)\right), \quad (6)$$

where  $L$  is the final layer and  $W$  projects the query hidden state to the vocabulary.

### 3.2 MULTI-STAGE TRAINING WITH PROGRESSIVE TOKEN GROUPING

Building on the connection between standard AR and A3, we design a progressive adaptation strategy that smoothly transitions from left-to-right generation to fully flexible any-order prediction. To leverage the stability and strong initialization of existing AR models, we begin training A3 from a pretrained AR checkpoint and gradually relax its constraints through three stages:

- **Stage 1: AR Initialization.** We align A3 with conventional AR training by setting the two-stream causal masks to exactly reproduce left-to-right factorization (Figure 2 Stage 1). Formally, the sequence  $x_{1:N}$  is partitioned into singleton groups:

$$G_1 = \{1\}, G_2 = \{2\}, \dots, G_N = \{N\}. \quad (7)$$

270 This ensures that  $P(x_{1:N}) = \prod_{t=1}^N P(x_t \mid x_{<t})$ , identical to standard AR, providing a  
 271 stable initialization.  
 272

- 273 • **Stage 2: Group Expansion.** We expand beyond token-level prediction by allowing groups  
 274 of size greater than one (Figure 2 Stage 2). Concretely, the sequence is partitioned into  
 275 contiguous segments of fixed size  $s > 1$ , e.g.,

$$276 \quad G_1 = \{1, \dots, s\}, \quad G_2 = \{s+1, \dots, 2s\}, \quad \dots \quad (8)$$

277 with  $s$  gradually increased from 1 to 4. This teaches the model to predict multiple tokens  
 278 jointly within each group while still maintaining AR dependencies across groups.  
 279

- 280 • **Stage 3: Order Permutation.** We introduce any-order prediction within groups (Figure 2  
 281 Stage 3). The group structure  $G_1, G_2, \dots, G_K$  remains sequential, but the token indices  
 282 assigned to each group are drawn from a random permutation of  $\{1, \dots, N\}$ . For example,  
 283 if  $\pi$  is a random permutation of indices, then

$$284 \quad G_1 = \{\pi(1), \dots, \pi(s)\}, \quad G_2 = \{\pi(s+1), \dots, \pi(2s)\}, \quad \dots \quad (9)$$

285 The model therefore learns to predict tokens in arbitrary subsets, while still preserving a  
 286 group-to-group AR factorization:  
 287

$$288 \quad P(x_{1:N}) = \prod_{k=1}^K P(x_{G_k} \mid x_{G_{<k}}). \quad (10)$$

292 This exposes the model to diverse intra-group orderings and enables it to generalize to  
 293 arbitrary prediction targets at inference.  
 294

295 By the end of this curriculum, the model is able to predict arbitrary subsets of tokens as coherent  
 296 groups while preserving the recursive dependency structure of AR. Importantly, at every stage of  
 297 training, each token in the sequence belongs to exactly one group, so all tokens are always predicted,  
 298 maximizing the learning signal and computational efficiency.

### 3.3 FLEXIBLE INFERENCE VIA GROUPWISE DECODING

301 Building on the A3 formulation, we propose flexible inference strategies that extend beyond conventional AR decoding. The first decoding method we introduce is **groupwise AR sampling**, which  
 302 generalizes standard left-to-right generation by sampling groups of tokens sequentially rather than  
 303 strictly one-by-one. Formally, let the token positions of a sequence be partitioned into  $K$  groups  
 304  $\mathcal{G} = \{G_1, G_2, \dots, G_K\}$ , where  $G_k \subseteq \{1, \dots, n\}$  and  $\bigcup_{k=1}^K G_k = \{1, \dots, n\}$ . Given a prompt  
 305 covering groups  $G_1, \dots, G_{k_0}$ , the model generates subsequent groups by conditioning on all pre-  
 306 ceding groups:  
 307

$$308 \quad p_\theta(x_{G_{k_0+1}}, \dots, x_{G_K} \mid x_{G_{\leq k_0}}) = \prod_{k=k_0+1}^K p_\theta(x_{G_k} \mid x_{G_{<k}}). \quad (11)$$

311 Here,  $x_{G_k}$  denotes the tokens within group  $G_k$ , and  $x_{G_{<k}}$  the tokens of all earlier groups. This  
 312 reduces to the classical AR factorization when  $|G_k| = 1$  for all  $k$ , but naturally generalizes to larger  
 313 groups. The procedure is summarized in Algorithm 1. Concretely, several grouping strategies can  
 314 be applied:  
 315

- 316 1. **Token-wise grouping.** Each token is treated as its own group, i.e.,  $G_k = \{k\}$ . The  
 317 decoding reduces to the standard left-to-right AR generation:

$$319 \quad p_\theta(x_1, \dots, x_n) = \prod_{t=1}^n p_\theta(x_t \mid x_{<t}). \quad (12)$$

- 322 2. **Fixed-size grouping.** Tokens are partitioned into groups of size  $s$ , e.g.,  $G_k = \{(k-1)s +$   
 323  $1, \dots, ks\}$  for  $s \in \{2, 4\}$ . In this case, the model predicts  $s$  tokens jointly per step and  
 324 accelerates decoding.

324        3. **Task-specific grouping.** For infilling tasks we allow groups to be arbitrary index subsets  
 325        and then assign group ids so that groups containing masked positions are decoded after  
 326        groups used as context. Concretely, let the sequence be partitioned into left, middle and  
 327        right index sets  $L, M, R$  (so  $\{1, \dots, n\} = L \cup M \cup R$ ). We choose an index  $k_0$  such that  
 328        every group  $G_k$  satisfying  $G_k \cap M = \emptyset$  has  $k \leq k_0$ , while every group that contains any  
 329        masked position satisfies  $k > k_0$  (groups need not be contiguous and a single group may  
 330        contain tokens from both  $L$  and  $R$ ). Under this design, all context groups (those covering  
 331         $L$  and  $R$ ) appear before the masked groups, and the model performs:

332        
$$p_{\theta}(x_M \mid x_{G_{\leq k_0}}) = \prod_{k=k_0+1}^K p_{\theta}(x_{G_k} \mid x_{G_{<k}}), \quad (13)$$
  
 333  
 334

335        which realizes AR dependencies inside each masked group while conditioning on both left  
 336        and right contexts. This flexible assignment enables infilling where context groups are  
 337        formed from arbitrary subsets of  $L \cup R$ , and masked spans are predicted group-by-group.  
 338        This capability distinguishes A3 from conventional AR models, which cannot directly con-  
 339        dition on future context during generation.

340        **Dynamic Resampling Inference.** Beyond fixed grouping, A3 also supports a more adaptive in-  
 341        ference procedure inspired by iterative refinement (Li et al., 2022; Chen et al., 2024a). Here, the  
 342        grouping  $\mathcal{G}$  is not fixed. At each step, the model evaluates all unfinished positions simultaneously,  
 343        conditioned on the completed tokens. Formally, suppose  $U_t \subseteq \{1, \dots, n\}$  is the set of unfinished  
 344        (blank) positions at iteration  $t$ , and  $F_t$  is its complement of finished positions. The model computes  
 345        predictive distributions

$$p_{\theta}(x_i \mid x_{F_t}), \quad \forall i \in U_t. \quad (14)$$

346        Based on these distributions, we then select a subset  $S_t \subseteq U_t$  to be committed at this step, according  
 347        to some criterion such as maximum confidence, lowest entropy (Kim et al., 2025), or simply random  
 348        sampling. Once  $S_t$  is chosen, the tokens at  $S_t$  are sampled and added to the finished set:

$$F_{t+1} = F_t \cup S_t, \quad U_{t+1} = U_t \setminus S_t. \quad (15)$$

349        This process repeats until  $U_T = \emptyset$ , at which point the sequence is fully generated. The procedure is  
 350        summarized in Algorithm 2. The advantage of this dynamic resampling strategy is twofold. First, it  
 351        allows the model to adaptively choose the granularity of generation based on prediction confidence,  
 352        committing to easy tokens early while deferring more uncertain positions until later. Second, unlike  
 353        diffusion-style denoising which follows a pre-specified noise schedule, A3 inference directly uses  
 354        the conditional distributions defined by the AR factorization, ensuring consistency between training  
 355        and inference.

356        These inference strategies highlight a trade-off between efficiency and flexibility. Fixed-group sam-  
 357        pling is fast but less adaptive, as performance depends on group alignment with text structure. Dy-  
 358        namic resampling is slower since all unfinished positions are reevaluated at each step, but it yields  
 359        greater accuracy by adapting token commitment to model confidence. We will compare these strate-  
 360        gies in the next section on real-world tasks.

## 4 EXPERIMENTS

### 4.1 SETUP

361        **Training Setup.** We initialize our models from the LLaMA series, including LLaMA-3.1-8B,  
 362        LLaMA-3.2-3B, and LLaMA-3.2-1B (Dubey et al., 2024). For training data, we construct a mixture  
 363        of the FineWeb dataset (Penedo et al., 2024) and the SlimPajama dataset (Soboleva et al., 2023),  
 364        following prior work on DLMs and AR models. From this mixture, we sample 2B tokens and  
 365        apply sequence packing with a maximum context length of 2048. All models are trained with full-  
 366        parameter fine-tuning in  $\text{bf16}$ . In the progressive adaptation recipe, the first two training stages are  
 367        trained for one epoch over 20% of the dataset, while the final stage is trained for one epoch over the  
 368        full dataset. Additional training details are provided in Appendix A.

369        **Evaluation Setup.** We adopt the evaluation protocol of Gong et al. (2025) to compare our mod-  
 370        els against both diffusion and AR baselines. For reading comprehension, we evaluate on TriviaQA

378

379

380

---

**Algorithm 1** Groupwise AR Sampling
 

---

**Require:** Prompt tokens  $x_{1:m}$ , grouping strategy  $\mathcal{G} = \{G_1, G_2, \dots, G_K\}$ , model  $f_\theta$   
**Ensure:** Generated sequence  $\hat{x}_{1:n}$ 

- 1: Initialize  $\hat{x}_{1:m} \leftarrow x_{1:m}$
- 2: Find the last group index  $k_0$  in the prompt
- 3: **for**  $k = k_0 + 1$  to  $K$  **do**
- 4:   Compute context representation  $h \leftarrow f_\theta(\hat{x}_{G_{<k}})$
- 5:   Sample tokens  $\hat{x}_{G_k} \sim p_\theta(\cdot | h)$
- 6: **end for**
- 7: **return** Completed sequence  $\hat{x}_{1:n}$

---

394

395

(Joshi et al., 2017) using exact match accuracy. For commonsense reasoning, we consider Hellaswag (Zellers et al., 2019), Winogrande (Sakaguchi et al., 2020), SIQA (Sap et al., 2019), and PIQA (Bisk et al., 2020), all assessed by multiple-choice accuracy. For story infilling, we use ROC-Stories (Mostafazadeh et al., 2016) and report ROUGE scores (Lin, 2004). We compare against two categories of baselines: (a) the base AR model LLaMA-3.1-8B, and (b) recent diffusion language models of varying sizes, including Plaid-1B (Gulrajani & Hashimoto, 2024), Dream-7B (Ye et al., 2025), and DiffuLlama-7B (Gong et al., 2025).

402

403

## 4.2 MAIN RESULTS

404

The results in Table 1 show that A3 consistently outperforms diffusion-based models across QA, commonsense reasoning, and infilling tasks. For example, A3-8B achieves 19.4 accuracy on TriviaQA and 78.1 on PIQA, surpassing all the diffusion baselines, while also attaining competitive ROUGE scores for story infilling. In fact, A3 also achieves better latency number on the infilling task (0.15 s/sample for A3 v.s. 0.17 s/sample for DiffuLlama and 0.21 s/sample for Llama-3.1-8B). These gains are particularly noteworthy given that A3 is trained on only 2B tokens, whereas DiffuLlama is trained on 65B. Although A3 still underperforms the AR baseline, this gap is likely attributable to limited training data; with larger-scale pretraining, we expect A3 to close the difference further.

413

Importantly, A3 demonstrates clear scaling behavior: performance improves steadily from 1B to 3B to 8B parameters, indicating that the method benefits from larger models in the same way as conventional AR training. Overall, these results confirm that A3 offers a favorable balance between AR and diffusion paradigms, combining strong reasoning accuracy with flexible generation, and holds promise for further improvements under larger-scale training.

418

419

## 4.3 ABLATION STUDY

420

**Inference Strategies.** To better understand the trade-offs between the two proposed inference strategies in Section 3.3, we conducted unconditional generation experiments under the A3 decoding framework. For groupwise AR sampling, we vary the group size from 1 to 4. For dynamic resampling, we vary the group size from 1 to 16 and implemented two selection criteria: (1) Confidence-based: selecting positions with highest maximum softmax probability. (2) Entropy-based: selecting positions with minimum output entropy. For each sequence, we sample with temperature of 1.5 and top-p of 0.95. Figure 3 reports the log of perplexity measured by Llama-3.1-8B and the average decoding time for one sequence.

429

430

431

We observe that dynamic resampling methods consistently achieve lower perplexity than groupwise AR sampling, indicating that they produce higher-quality generations. The confidence-based and entropy-based criteria yield very similar performance, with confidence being slightly better at smaller group sizes. However, all strategies show a trend of increasing perplexity as group size

378

379

380

---

**Algorithm 2** Dynamic Resampling
 

---

**Require:** : Prompt tokens, model  $f_\theta$ , criterion
 

- 1: Initialize  $F_0$  with prompt tokens,  $U_0$  with blank positions
- 2: **while**  $U_t \neq \emptyset$  **do**
- 3:   **for** each  $i \in U_t$  **do**
- 4:     Compute  $p_\theta(x_i | x_{F_t})$
- 5:   **end for**
- 6:   Select subset  $S_t \subseteq U_t$  based on criterion
- 7:   **for** each  $i \in S_t$  **do**
- 8:     Sample  $\hat{x}_i \sim p_\theta(x_i | x_{F_t})$
- 9:   **end for**
- 10:   Update  $F_{t+1} \leftarrow F_t \cup S_t$ ,  $U_{t+1} \leftarrow U_t \setminus S_t$
- 11: **end while**
- 12: **return** Completed sequence  $x_{1:n}$

---

432  
 433 Table 1: Comprehensive evaluation of different language models. There are 4 types of these models:  
 434 AR for autoregressive, DD for discrete diffusion, CD for continuous diffusion and A3 for our pro-  
 435 posed model. For the infilling task, we use ROUGE-1/2/L score; for other tasks, we use the accuracy  
 436 (%) metric. \* refers to the results reported in DiffuLlama (Gong et al., 2025).

437 Model	438 Size	439 Type	440 QA TriQA	441 CommonSense Reasoning			442 Infilling	
				443 HSwag	444 Wino.	445 SIQA	446 PIQA	447 ROCStories
Llama-3.1	8B	AR	52.1	76.0	63.9	46.7	80.3	11.7/2.3/10.5
Plaid*	1B	CD	1.2	39.3	51.3	32.3	54.5	12.1/1.1/11.2
Dream	7B	DD	18.3	26.9	51.8	36.6	55.8	11.7/2.3/10.5
DiffuLlama*	7B	DD	18.5	<b>58.7</b>	56.4	43.2	63.3	<b>23.3/5.5/21.2</b>
	1B	A3	10.2	40.2	52.8	35.1	64.7	11.8/1.7/11.1
A3	3B	A3	15.9	49.6	54.3	38.9	70.1	11.3/2.3/10.2
	8B	A3	<b>19.4</b>	58.4	<b>60.2</b>	<b>45.2</b>	<b>78.1</b>	19.2/4.6/18.6

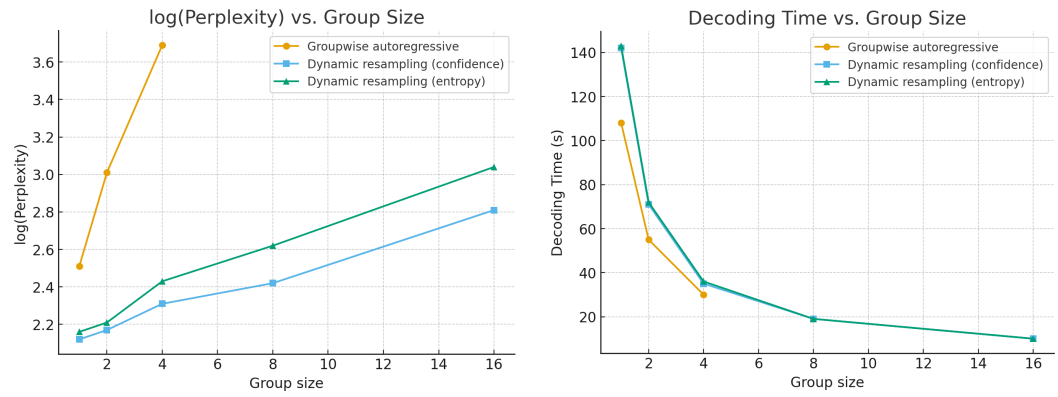


Figure 3: Unconditional generation log(perplexity) and speed using A3-8B. The perplexity is measured by Llama-3.1-8B and we compare several decoding strategies. Dynamic resampling will cost more time but have lower perplexity.

grows, reflecting the trade-off between decoding granularity and modeling accuracy. We can also see that decoding time decreases sharply with larger group sizes. Groupwise AR sampling is fastest at the same group size because it only generates the designated group per step, while dynamic resampling requires evaluating all unfinished tokens at each iteration, making it slower. However, as group size increases, dynamic resampling speeds up considerably, nearly matching the efficiency of groupwise sampling at large group sizes.

Overall, these results demonstrate a speed–accuracy trade-off. Groupwise AR sampling is faster but less accurate, while dynamic resampling achieves better perplexity at the cost of slower decoding. Importantly, A3 provides the flexibility to choose between these strategies depending on the requirements of the application, making it more flexible than conventional AR or diffusion-based methods.

**Curriculum schedule.** A3 introduces a different causal mask and attention flow from a standard AR transformer, and the model must progressively adapt from strict left-to-right prediction to multi-token and eventually arbitrary-order factorization. To assess the sensitivity of the schedule, we train two variants on 0.5B tokens: 1. original curriculum, and 2. skipping stage 1 and 2 (directly training on stage 3: order permutations). Results are shown in Table 2. Skipping the early stages consistently hurts performance by 4–6 points on several benchmarks, which proves the importance of such adaptation stage. An adaptive schedule, e.g., based on training loss, may further improve robustness. We plan to investigate this direction in the future work.

**Performance with more data.** Since the training budget for A3 is much less than the baseline (2B for A3, 60B for DiffuLlama and 15T for Llama-3.1-8B), in order to isolate the architecture effect on the worse performance than the AR baseline, we track how A3 improves under increasing post-

486  
 487 Table 2: Performance with different training curriculum schedule. We evaluate two variants trained  
 488 on 0.5B tokens: 1. original curriculum and, 2. skipping stage 1 and 2 (directly training on stage 3:  
 489 order permutations).

490 491 Schedule	492 QA			493 CommonSense Reasoning		494 Infilling
	495 TriQA	496 HSwag	497 Wino.	498 SIQA	499 PIQA	500 ROCStories
Original	<b>15.6</b>	<b>49.3</b>	<b>56.7</b>	<b>39.6</b>	<b>69.4</b>	<b>13.2/2.3/12.6</b>
Skipping Stage 1 & 2	11.3	44.2	54.1	37.3	64.2	13.1/2.2/12.4

495  
 496 Table 3: Performance of A3 with different training data  
 497 on TriviaQA and perplexity measured by Llama-3.1-8B.

500 Model	501 TriviaQA	502 log(Perplexity)
A3 (1.5B tokens)	16.2	2.9
A3 (2B tokens)	19.4	2.5
A3 (2.5B tokens)	22.5	2.3
AR (15T)	52.1	0.8

Table 4: Model loss of A3 across context  
 lengths, which is stably small.

Length	Model loss
256	3.54
512	3.51
1024	3.34
2048	3.23

505  
 506 training data. We use 1.5B, 2B (default) and 2.5B tokens to train A3. The results are shown in Table  
 507 3. Performance increases steadily with more data. This confirms that A3 benefits strongly from data  
 508 scale and that the gap to fully-trained AR models is due to training budget, not a limitation of the  
 509 A3 architecture.

510  
 511 **Robustness on context length.** In order to investigate whether A3 is robust across different context  
 512 lengths, we input contexts with length of 512, 1024 and 2048 to A3 and calculate the loss. The  
 513 results are shown in Table 4. The model loss keeps stable within the training length, indicating the  
 514 robustness of A3 across different context lengths.

## 5 CONCLUSION

517  
 518 We have presented Any-order Any-subset Autoregressive modeling (A3), a novel framework that  
 519 generalizes traditional autoregressive factorization to enable flexible, groupwise generation of to-  
 520 kens in arbitrary orders. By combining a two-stream attention architecture with a progressive train-  
 521 ing strategy, A3 achieves the dual goals of generation flexibility and modeling stability. Our ap-  
 522 proach supports a wide range of decoding strategies, including groupwise autoregressive sampling  
 523 and dynamic resampling, offering a tunable trade-off between speed and accuracy. Through com-  
 524 prehensive experiments, we demonstrate that A3 outperforms diffusion-based models in reasoning,  
 525 question answering, and infilling tasks. These results highlight A3’s ability to balance efficiency,  
 526 flexibility, and quality, making it a promising direction for future sequence modeling. In the fu-  
 527 ture, we plan to explore scaling A3 to larger models and datasets, as well as applying it to more  
 528 challenging tasks such as long-context reasoning.

## 529 ETHICS STATEMENT

531  
 532 This work complies with the ICLR Code of Ethics. While our methods are general, they may be  
 533 applied in contexts with societal implications, including risks related to bias, fairness, and privacy.  
 534 We encourage responsible use and declare no conflicts of interest.

## 535 REPRODUCIBILITY STATEMENT

536  
 537 We provide detailed descriptions of our methodology, datasets, model configurations, and eval-  
 538 uation metrics in both the main text and the Appendix. Codes will be released upon accep-  
 539 tance.

540 REFERENCES  
541

542 Jacob Austin, Daniel D Johnson, Jonathan Ho, Daniel Tarlow, and Rianne Van Den Berg. Structured  
543 denoising diffusion models in discrete state-spaces. *Advances in neural information processing*  
544 *systems*, 34:17981–17993, 2021. 3, 15

545 Jinze Bai, Shuai Bai, Yunfei Chu, Zeyu Cui, Kai Dang, Xiaodong Deng, Yang Fan, Wenbin Ge,  
546 Yu Han, Fei Huang, et al. Qwen technical report. *arXiv preprint arXiv:2309.16609*, 2023a. 1, 2  
547

548 Yushi Bai, Xin Lv, Jiajie Zhang, Hongchang Lyu, Jiankai Tang, Zhidian Huang, Zhengxiao Du,  
549 Xiao Liu, Aohan Zeng, Lei Hou, et al. Longbench: A bilingual, multitask benchmark for long  
550 context understanding. *arXiv preprint arXiv:2308.14508*, 2023b. 1, 17, 18

551 Yonatan Bisk, Rowan Zellers, Jianfeng Gao, Yejin Choi, et al. Piqa: Reasoning about physical  
552 commonsense in natural language. In *AAAI*, 2020. 1, 8  
553

554 Tianle Cai, Yuhong Li, Zhengyang Geng, Hongwu Peng, Jason D Lee, Deming Chen, and Tri  
555 Dao. Medusa: Simple llm inference acceleration framework with multiple decoding heads. *arXiv*  
556 *preprint arXiv:2401.10774*, 2024. 16

557 Pinzhen Chen, Zhicheng Guo, Barry Haddow, and Kenneth Heafield. Iterative translation refinement  
558 with large language models. In *EAMT*, 2024a. 7  
559

560 Yukang Chen, Shengju Qian, Haotian Tang, Xin Lai, Zhijian Liu, Song Han, and Jiaya Jia. Lon-  
561 gloRA: Efficient fine-tuning of long-context large language models. In *ICLR*, 2024b. 15

562 Sander Dieleman, Laurent Sartran, Arman Roshannai, Nikolay Savinov, Yaroslav Ganin, Pierre H  
563 Richemond, Arnaud Doucet, Robin Strudel, Chris Dyer, Conor Durkan, et al. Continuous diffu-  
564 sion for categorical data. *arXiv preprint arXiv:2211.15089*, 2022. 15  
565

566 Abhimanyu Dubey, Abhinav Jauhri, Abhinav Pandey, Abhishek Kadian, Ahmad Al-Dahle, Aiesha  
567 Letman, Akhil Mathur, Alan Schelten, Amy Yang, Angela Fan, et al. The llama 3 herd of models.  
568 *arXiv e-prints*, pp. arXiv–2407, 2024. 7

569 Yao Fu, Rameswar Panda, Xinyao Niu, Xiang Yue, Hannaneh Hajishirzi, Yoon Kim, and Hao Peng.  
570 Data engineering for scaling language models to 128k context. *arXiv preprint arXiv:2402.10171*,  
571 2024. 15  
572

573 Fabian Gloeckle, Badr Youbi Idrissi, Baptiste Rozière, David Lopez-Paz, and Gabriel Synnaeve.  
574 Better & faster large language models via multi-token prediction. In *ICML*, 2024. 3

575 Shanshan Gong, Mukai Li, Jiangtao Feng, Zhiyong Wu, and LingPeng Kong. Diffuseq: Sequence to  
576 sequence text generation with diffusion models. *arXiv preprint arXiv:2210.08933*, 2022. 15, 16  
577

578 Shanshan Gong, Shivam Agarwal, Yizhe Zhang, Jiacheng Ye, Lin Zheng, Mukai Li, Chenxin An,  
579 Peilin Zhao, Wei Bi, Jiawei Han, et al. Scaling diffusion language models via adaptation from  
580 autoregressive models. In *ICLR*, 2025. 1, 2, 3, 7, 8, 9, 15

581 Jiatao Gu, James Bradbury, Caiming Xiong, Victor OK Li, and Richard Socher. Non-autoregressive  
582 neural machine translation. *arXiv preprint arXiv:1711.02281*, 2017. 15  
583

584 Jiatao Gu, Changhan Wang, and Junbo Zhao. Levenshtein transformer. *Advances in neural infor-*  
585 *mation processing systems*, 32, 2019. 16

586 Ishaan Gulrajani and Tatsunori B Hashimoto. Likelihood-based diffusion language models. In  
587 *NeurIPS*, 2024. 1, 2, 8, 15

588 Gabe Guo and Stefano Ermon. Reviving any-subset autoregressive models with principled parallel  
589 sampling and speculative decoding. *arXiv preprint arXiv:2504.20456*, 2025. 17  
590

591 Junliang Guo, Xu Tan, Linli Xu, Tao Qin, Enhong Chen, and Tie-Yan Liu. Fine-tuning by cur-  
592 riculum learning for non-autoregressive neural machine translation. In *Proceedings of the AAAI*  
593 *Conference on Artificial Intelligence*, volume 34, pp. 7839–7846, 2020. 16

594 Suchin Gururangan, Ana Marasović, Swabha Swamyamdipta, Kyle Lo, Iz Beltagy, Doug Downey,  
 595 and Noah A Smith. Don't stop pretraining: Adapt language models to domains and tasks. *arXiv*  
 596 *preprint arXiv:2004.10964*, 2020. 15

597

598 Xiaochuang Han, Sachin Kumar, and Yulia Tsvetkov. Ssd-lm: Semi-autoregressive simplex-  
 599 based diffusion language model for text generation and modular control. *arXiv preprint*  
 600 *arXiv:2210.17432*, 2022. 15, 16

601 Zhengfu He, Tianxiang Sun, Qiong Tang, Kuanning Wang, Xuan-Jing Huang, and Xipeng Qiu.  
 602 Diffusionbert: Improving generative masked language models with diffusion models. In *ACL*,  
 603 2023. 3

604

605 Yosuke Higuchi, Shinji Watanabe, Nanxin Chen, Tetsuji Ogawa, and Tetsunori Kobayashi.  
 606 Mask ctc: Non-autoregressive end-to-end asr with ctc and mask predict. *arXiv preprint*  
 607 *arXiv:2005.08700*, 2020. 16

608 Jonathan Ho, Ajay Jain, and Pieter Abbeel. Denoising diffusion probabilistic models. In *NeurIPS*,  
 609 2020. 15

610

611 Emiel Hoogeboom, Didrik Nielsen, Priyank Jaini, Patrick Forré, and Max Welling. Argmax flows  
 612 and multinomial diffusion: Learning categorical distributions. In *NeurIPS*, 2021. 15

613 Mandar Joshi, Eunsol Choi, Daniel S Weld, and Luke Zettlemoyer. Triviaqa: A large scale distantly  
 614 supervised challenge dataset for reading comprehension. In *ACL*, 2017. 1, 8

615

616 Zixuan Ke, Yijia Shao, Haowei Lin, Tatsuya Konishi, Gyuhak Kim, and Bing Liu. Continual pre-  
 617 training of language models. In *ICLR*, 2023. 15

618 Jaeyeon Kim, Kulin Shah, Vasilis Kontonis, Sham M Kakade, and Sitan Chen. Train for the worst,  
 619 plan for the best: Understanding token ordering in masked diffusions. In *ICML*, 2025. 1, 2, 7

620

621 Siqi Kou, Lanxiang Hu, Zhezhi He, Zhijie Deng, and Hao Zhang. Cllms: consistency large language  
 622 models. In *ICML*, 2024. 3

623

624 Yury Kuratov, Aydar Bulatov, Petr Anokhin, Ivan Rodkin, Dmitry Sorokin, Artyom Sorokin, and  
 625 Mikhail Burtsev. Babilong: Testing the limits of llms with long context reasoning-in-a-haystack.  
 626 *NeurIPS*, 2024. 1

627 Jason Lee, Elman Mansimov, and Kyunghyun Cho. Deterministic non-autoregressive neural se-  
 628 quence modeling by iterative refinement. *arXiv preprint arXiv:1802.06901*, 2018. 16

629

630 Yaniv Leviathan, Matan Kalman, and Yossi Matias. Fast inference from transformers via speculative  
 631 decoding. In *ICML*, 2023. 16

632

633 Xiang Li, John Thickstun, Ishaan Gulrajani, Percy S Liang, and Tatsunori B Hashimoto. Diffusion-  
 634 lm improves controllable text generation. In *NeurIPS*, 2022. 1, 2, 3, 7, 15

635

636 Yuhui Li, Fangyun Wei, Chao Zhang, and Hongyang Zhang. Eagle: Speculative sampling requires  
 637 rethinking feature uncertainty. *arXiv preprint arXiv:2401.15077*, 2024. 16

638

639 Chin-Yew Lin. Rouge: A package for automatic evaluation of summaries. In *Text summarization  
 branches out*, pp. 74–81, 2004. 8

640

641 Aaron Lou, Chenlin Meng, and Stefano Ermon. Discrete diffusion language modeling by estimating  
 642 the ratios of the data distribution. *arXiv preprint arXiv:2310.16834*, 2023. 15, 16

643

644 Nasrin Mostafazadeh, Nathanael Chambers, Xiaodong He, Devi Parikh, Dhruv Batra, Lucy Vander-  
 645 wende, Pushmeet Kohli, and James Allen. A corpus and cloze evaluation for deeper understanding  
 646 of commonsense stories. In *NAACL*, 2016. 1, 8

647

648 Shen Nie, Fengqi Zhu, Zebin You, Xiaolu Zhang, Jingyang Ou, Jun Hu, JUN ZHOU, Yankai Lin,  
 649 Ji-Rong Wen, and Chongxuan Li. Large language diffusion models. In *ICLR 2025 Workshop on  
 650 Deep Generative Model in Machine Learning: Theory, Principle and Efficacy*, 2025. 3

648 Jingyang Ou, Shen Nie, Kaiwen Xue, Fengqi Zhu, Jiacheng Sun, Zhenguo Li, and Chongxuan  
 649 Li. Your absorbing discrete diffusion secretly models the conditional distributions of clean data.  
 650 *arXiv preprint arXiv:2406.03736*, 2024. 15

651 Guilherme Penedo, Hynek Kydlíček, Anton Lozhkov, Margaret Mitchell, Colin A Raffel, Leandro  
 652 Von Werra, Thomas Wolf, et al. The fineweb datasets: Decanting the web for the finest text data  
 653 at scale. In *NeurIPS*, 2024. 7

654 Alec Radford, Karthik Narasimhan, Tim Salimans, Ilya Sutskever, et al. Improving language under-  
 655 standing by generative pre-training. 2018. 1, 2

656 Jack W Rae, Anna Potapenko, Siddhant M Jayakumar, and Timothy P Lillicrap. Compressive  
 657 transformers for long-range sequence modelling. *arXiv preprint arXiv:1911.05507*, 2019. 17

658 Subham Sahoo, Marianne Arriola, Yair Schiff, Aaron Gokaslan, Edgar Marroquin, Justin Chiu,  
 659 Alexander Rush, and jiuVolodymyr Kuleshov. Simple and effective masked diffusion language  
 660 models. In *NeurIPS*, 2024. 15

661 Keisuke Sakaguchi, Ronan Le Bras, Chandra Bhagavatula, and Yejin Choi. Winogrande: An adver-  
 662 sarial winograd schema challenge at scale. In *AAAI*, 2020. 1, 8

663 Mohammad Samragh, Iman Mirzadeh, Keivan Alizadeh Vahid, Fartash Faghri, Minsik Cho, Moin  
 664 Nabi, Devang Naik, and Mehrdad Farajtabar. Scaling smart: Accelerating large language model  
 665 pre-training with small model initialization. *arXiv preprint arXiv:2409.12903*, 2024. 15

666 Maarten Sap, Hannah Rashkin, Derek Chen, Ronan LeBras, and Yejin Choi. Socialiqa: Common-  
 667 sense reasoning about social interactions. In *EMNLP*, 2019. 1, 8

668 Tianxiao Shen, Hao Peng, Ruoqi Shen, Yao Fu, Zaid Harchaoui, and Yejin Choi. Film: Fill-in  
 669 language models for any-order generation. *arXiv preprint arXiv:2310.09930*, 2023. 16

670 Daria Soboleva, Faisal Al-Khateeb, Robert Myers, Jacob R Steeves, Joel Hestness, and Nolan Dey.  
 671 SlimPajama: A 627B token cleaned and deduplicated version of RedPajama, 2023. URL <https://huggingface.co/datasets/cerebras/SlimPajama-627B>. 7

672 Jascha Sohl-Dickstein, Eric Weiss, Niru Maheswaranathan, and Surya Ganguli. Deep unsupervised  
 673 learning using nonequilibrium thermodynamics. In *ICML*, 2015. 15

674 Yang Song, Jascha Sohl-Dickstein, Diederik P Kingma, Abhishek Kumar, Stefano Ermon, and Ben  
 675 Poole. Score-based generative modeling through stochastic differential equations. *arXiv preprint  
 676 arXiv:2011.13456*, 2020. 15

677 Mitchell Stern, Noam Shazeer, and Jakob Uszkoreit. Blockwise parallel decoding for deep autore-  
 678 gressive models. *Advances in Neural Information Processing Systems*, 31, 2018. 16

679 Mitchell Stern, William Chan, Jamie Kiros, and Jakob Uszkoreit. Insertion transformer: Flexible  
 680 sequence generation via insertion operations. In *International Conference on Machine Learning*,  
 681 pp. 5976–5985. PMLR, 2019. 16

682 Hugo Touvron, Louis Martin, Kevin Stone, Peter Albert, Amjad Almahairi, Yasmine Babaei, Niko-  
 683 lay Bashlykov, Soumya Batra, Prajjwal Bhargava, Shruti Bhosale, et al. Llama 2: Open founda-  
 684 tion and fine-tuned chat models. *arXiv preprint arXiv:2307.09288*, 2023. 1, 2

685 Wenhan Xiong, Jingyu Liu, Igor Molybog, Hejia Zhang, Prajjwal Bhargava, Rui Hou, Louis Martin,  
 686 Rashi Rungta, Karthik Abinav Sankararaman, Barlas Oguz, et al. Effective long-context scaling  
 687 of foundation models. *arXiv preprint arXiv:2309.16039*, 2023. 15

688 Yiheng Xu, Hongjin SU, Chen Xing, Boyu Mi, Qian Liu, Weijia Shi, Binyuan Hui, Fan Zhou, Yitao  
 689 Liu, Tianbao Xie, Zhoujun Cheng, Siheng Zhao, Lingpeng Kong, Bailin Wang, Caiming Xiong,  
 690 and Tao Yu. Lemur: Harmonizing natural language and code for language agents. In *ICLR*, 2024.  
 691 15

692 Zhilin Yang, Zihang Dai, Yiming Yang, Jaime Carbonell, Russ R Salakhutdinov, and Quoc V Le.  
 693 Xlnet: Generalized autoregressive pretraining for language understanding. In *NeurIPS*, 2019. 3,  
 694 4, 16

702 Jiacheng Ye, Zhihui Xie, Lin Zheng, Jiahui Gao, Zirui Wu, Xin Jiang, Zhenguo Li, and Lingpeng  
703 Kong. Dream 7b: Diffusion large language models. *arXiv preprint arXiv:2508.15487*, 2025. 8  
704

705 Rowan Zellers, Ari Holtzman, Yonatan Bisk, Ali Farhadi, and Yejin Choi. Hellaswag: Can a ma-  
706 chine really finish your sentence? In *ACL*, 2019. 1, 8

707 Lin Zheng, Jianbo Yuan, Lei Yu, and Lingpeng Kong. A reparameterized discrete diffusion model  
708 for text generation. In *COLM*, 2024. 15  
709

710

711

712

713

714

715

716

717

718

719

720

721

722

723

724

725

726

727

728

729

730

731

732

733

734

735

736

737

738

739

740

741

742

743

744

745

746

747

748

749

750

751

752

753

754

755

756 **A TRAINING HYPERPARAMETERS**  
757758 We list the hyperparameters in the training stage in Table 5  
759760 Table 5: The hyperparameter list  
761

762 Hyperparameter	763 Value
<i>Training</i>	
764 Batch Size	765 64
766 Epoch	767 [0.2, 0.2, 1]
768 Optimizer	769 AdamW
770 LR	771 2e-5
772 Betas	773 (0.9, 0.999)
774 Weight Decay	775 0.01
776 LR Schedule	777 WarmupLR
778 Warmup Iters	779 [50, 50, 50]
780 Max Sequence Length	781 2048
<i>Sampling (Section 4.3)</i>	
782 Top-p	783 0.95
784 Temperature	785 1.5

786 **B ADDITIONAL RELATED WORK**  
787788 **Continue Pre-training.** Pretraining large language models has been proven to be complex and  
789 computationally expensive (Samragh et al., 2024). Consequently, continued pre-training has been  
790 proposed as an effective method to adapt existing large language models to specific domains (Ke  
791 et al., 2023; Gururangan et al., 2020) or to endow them with new capabilities, such as handling  
792 longer contexts (Chen et al., 2024b; Fu et al., 2024; Xiong et al., 2023) or code generation (Xu et al.,  
793 2024). Notably, certain continued pre-training efforts, such as those in scaling diffusion language  
794 models (Gong et al., 2025), have transcended autoregressive (AR) language modeling by converting  
795 large language models into diffusion-based architectures, thereby enabling parallel token genera-  
796 tion. In contrast, our work retains autoregressive language modeling but innovatively incorporates a  
797 two-stream architecture and semi-autoregressive decoding to similarly support parallel prediction of  
798 multiple tokens, achieving significant reductions in inference latency compared to both autoregres-  
799 sive and diffusion-based baselines.  
800801 **Diffusion Language Model.** Diffusion models (Sohl-Dickstein et al., 2015; Ho et al., 2020; Song  
802 et al., 2020) have demonstrated remarkable capabilities in image generation. Consequently, a series  
803 of works have sought to extend diffusion models to text generation, which can be roughly divided  
804 into the continuous diffusion model and the discrete diffusion model. One straightforward approach  
805 involves embedding text data into a continuous space and directly applying diffusion models (Li  
806 et al., 2022; Gong et al., 2022; Han et al., 2022; Dieleman et al., 2022). However, the scalability  
807 of continuous diffusion methods remains a challenge, as they require substantially greater compu-  
808 tational cost compared to AR models to achieve equivalent performance (Gulrajani & Hashimoto,  
809 2024). To better accommodate the discrete nature of text, an alternative paradigm replaces con-  
810 tinuous diffusion with a discrete process, introducing an absorbing [MASK] state as noise (Austin  
811 et al., 2021; Hoogeboom et al., 2021; Zheng et al., 2024; Sahoo et al., 2024). Lou et al. (2023)  
812 demonstrated that masked diffusion models (MDMs) achieve perplexity comparable to or even sur-  
813 passing that of AR models at the GPT-2 scale. Ou et al. (2024) established foundational theoretical  
814 results, affirming the feasibility of MDMs. In comparison to MDMs, our method similarly enables  
815 parallel prediction of groups of tokens and leverages bidirectional context. However, by retaining  
816 autoregressive modeling, our approach utilizes every token during training, thereby facilitating faster  
817 convergence relative to MDMs.  
818819 **Non-autoregressive Generation.** Non-autoregressive (NAR) generation (Gu et al., 2017) accel-  
820 erates inference by producing target tokens in parallel, eliminating the dependency on previously  
821 generated tokens inherent in traditional AR models. This approach substantially improves genera-  
822

810  
 811  
 812  
 813  
 814  
 815  
 816  
 817  
 818  
 819  
 820  
 821  
 822  
 823  
 824  
 825  
 826  
 827  
 828  
 829  
 830  
 831  
 832  
 833  
 834  
 835  
 836  
 837  
 838  
 839  
 840  
 841  
 842  
 843  
 844  
 845  
 846  
 847  
 848  
 849  
 850  
 851  
 852  
 853  
 854  
 855  
 856  
 857  
 858  
 859  
 860  
 861  
 862  
 863  
 864  
 865  
 866  
 867  
 868  
 869  
 870  
 871  
 872  
 873  
 874  
 875  
 876  
 877  
 878  
 879  
 880  
 881  
 882  
 883  
 884  
 885  
 886  
 887  
 888  
 889  
 890  
 891  
 892  
 893  
 894  
 895  
 896  
 897  
 898  
 899  
 900  
 901  
 902  
 903  
 904  
 905  
 906  
 907  
 908  
 909  
 910  
 911  
 912  
 913  
 914  
 915  
 916  
 917  
 918  
 919  
 920  
 921  
 922  
 923  
 924  
 925  
 926  
 927  
 928  
 929  
 930  
 931  
 932  
 933  
 934  
 935  
 936  
 937  
 938  
 939  
 940  
 941  
 942  
 943  
 944  
 945  
 946  
 947  
 948  
 949  
 950  
 951  
 952  
 953  
 954  
 955  
 956  
 957  
 958  
 959  
 960  
 961  
 962  
 963  
 964  
 965  
 966  
 967  
 968  
 969  
 970  
 971  
 972  
 973  
 974  
 975  
 976  
 977  
 978  
 979  
 980  
 981  
 982  
 983  
 984  
 985  
 986  
 987  
 988  
 989  
 990  
 991  
 992  
 993  
 994  
 995  
 996  
 997  
 998  
 999  
 1000  
 1001  
 1002  
 1003  
 1004  
 1005  
 1006  
 1007  
 1008  
 1009  
 1010  
 1011  
 1012  
 1013  
 1014  
 1015  
 1016  
 1017  
 1018  
 1019  
 1020  
 1021  
 1022  
 1023  
 1024  
 1025  
 1026  
 1027  
 1028  
 1029  
 1030  
 1031  
 1032  
 1033  
 1034  
 1035  
 1036  
 1037  
 1038  
 1039  
 1040  
 1041  
 1042  
 1043  
 1044  
 1045  
 1046  
 1047  
 1048  
 1049  
 1050  
 1051  
 1052  
 1053  
 1054  
 1055  
 1056  
 1057  
 1058  
 1059  
 1060  
 1061  
 1062  
 1063  
 1064  
 1065  
 1066  
 1067  
 1068  
 1069  
 1070  
 1071  
 1072  
 1073  
 1074  
 1075  
 1076  
 1077  
 1078  
 1079  
 1080  
 1081  
 1082  
 1083  
 1084  
 1085  
 1086  
 1087  
 1088  
 1089  
 1090  
 1091  
 1092  
 1093  
 1094  
 1095  
 1096  
 1097  
 1098  
 1099  
 1100  
 1101  
 1102  
 1103  
 1104  
 1105  
 1106  
 1107  
 1108  
 1109  
 1110  
 1111  
 1112  
 1113  
 1114  
 1115  
 1116  
 1117  
 1118  
 1119  
 1120  
 1121  
 1122  
 1123  
 1124  
 1125  
 1126  
 1127  
 1128  
 1129  
 1130  
 1131  
 1132  
 1133  
 1134  
 1135  
 1136  
 1137  
 1138  
 1139  
 1140  
 1141  
 1142  
 1143  
 1144  
 1145  
 1146  
 1147  
 1148  
 1149  
 1150  
 1151  
 1152  
 1153  
 1154  
 1155  
 1156  
 1157  
 1158  
 1159  
 1160  
 1161  
 1162  
 1163  
 1164  
 1165  
 1166  
 1167  
 1168  
 1169  
 1170  
 1171  
 1172  
 1173  
 1174  
 1175  
 1176  
 1177  
 1178  
 1179  
 1180  
 1181  
 1182  
 1183  
 1184  
 1185  
 1186  
 1187  
 1188  
 1189  
 1190  
 1191  
 1192  
 1193  
 1194  
 1195  
 1196  
 1197  
 1198  
 1199  
 1200  
 1201  
 1202  
 1203  
 1204  
 1205  
 1206  
 1207  
 1208  
 1209  
 1210  
 1211  
 1212  
 1213  
 1214  
 1215  
 1216  
 1217  
 1218  
 1219  
 1220  
 1221  
 1222  
 1223  
 1224  
 1225  
 1226  
 1227  
 1228  
 1229  
 1230  
 1231  
 1232  
 1233  
 1234  
 1235  
 1236  
 1237  
 1238  
 1239  
 1240  
 1241  
 1242  
 1243  
 1244  
 1245  
 1246  
 1247  
 1248  
 1249  
 1250  
 1251  
 1252  
 1253  
 1254  
 1255  
 1256  
 1257  
 1258  
 1259  
 1260  
 1261  
 1262  
 1263  
 1264  
 1265  
 1266  
 1267  
 1268  
 1269  
 1270  
 1271  
 1272  
 1273  
 1274  
 1275  
 1276  
 1277  
 1278  
 1279  
 1280  
 1281  
 1282  
 1283  
 1284  
 1285  
 1286  
 1287  
 1288  
 1289  
 1290  
 1291  
 1292  
 1293  
 1294  
 1295  
 1296  
 1297  
 1298  
 1299  
 1300  
 1301  
 1302  
 1303  
 1304  
 1305  
 1306  
 1307  
 1308  
 1309  
 1310  
 1311  
 1312  
 1313  
 1314  
 1315  
 1316  
 1317  
 1318  
 1319  
 1320  
 1321  
 1322  
 1323  
 1324  
 1325  
 1326  
 1327  
 1328  
 1329  
 1330  
 1331  
 1332  
 1333  
 1334  
 1335  
 1336  
 1337  
 1338  
 1339  
 1340  
 1341  
 1342  
 1343  
 1344  
 1345  
 1346  
 1347  
 1348  
 1349  
 1350  
 1351  
 1352  
 1353  
 1354  
 1355  
 1356  
 1357  
 1358  
 1359  
 1360  
 1361  
 1362  
 1363  
 1364  
 1365  
 1366  
 1367  
 1368  
 1369  
 1370  
 1371  
 1372  
 1373  
 1374  
 1375  
 1376  
 1377  
 1378  
 1379  
 1380  
 1381  
 1382  
 1383  
 1384  
 1385  
 1386  
 1387  
 1388  
 1389  
 1390  
 1391  
 1392  
 1393  
 1394  
 1395  
 1396  
 1397  
 1398  
 1399  
 1400  
 1401  
 1402  
 1403  
 1404  
 1405  
 1406  
 1407  
 1408  
 1409  
 1410  
 1411  
 1412  
 1413  
 1414  
 1415  
 1416  
 1417  
 1418  
 1419  
 1420  
 1421  
 1422  
 1423  
 1424  
 1425  
 1426  
 1427  
 1428  
 1429  
 1430  
 1431  
 1432  
 1433  
 1434  
 1435  
 1436  
 1437  
 1438  
 1439  
 1440  
 1441  
 1442  
 1443  
 1444  
 1445  
 1446  
 1447  
 1448  
 1449  
 1450  
 1451  
 1452  
 1453  
 1454  
 1455  
 1456  
 1457  
 1458  
 1459  
 1460  
 1461  
 1462  
 1463  
 1464  
 1465  
 1466  
 1467  
 1468  
 1469  
 1470  
 1471  
 1472  
 1473  
 1474  
 1475  
 1476  
 1477  
 1478  
 1479  
 1480  
 1481  
 1482  
 1483  
 1484  
 1485  
 1486  
 1487  
 1488  
 1489  
 1490  
 1491  
 1492  
 1493  
 1494  
 1495  
 1496  
 1497  
 1498  
 1499  
 1500  
 1501  
 1502  
 1503  
 1504  
 1505  
 1506  
 1507  
 1508  
 1509  
 1510  
 1511  
 1512  
 1513  
 1514  
 1515  
 1516  
 1517  
 1518  
 1519  
 1520  
 1521  
 1522  
 1523  
 1524  
 1525  
 1526  
 1527  
 1528  
 1529  
 1530  
 1531  
 1532  
 1533  
 1534  
 1535  
 1536  
 1537  
 1538  
 1539  
 1540  
 1541  
 1542  
 1543  
 1544  
 1545  
 1546  
 1547  
 1548  
 1549  
 1550  
 1551  
 1552  
 1553  
 1554  
 1555  
 1556  
 1557  
 1558  
 1559  
 1560  
 1561  
 1562  
 1563  
 1564  
 1565  
 1566  
 1567  
 1568  
 1569  
 1570  
 1571  
 1572  
 1573  
 1574  
 1575  
 1576  
 1577  
 1578  
 1579  
 1580  
 1581  
 1582  
 1583  
 1584  
 1585  
 1586  
 1587  
 1588  
 1589  
 1590  
 1591  
 1592  
 1593  
 1594  
 1595  
 1596  
 1597  
 1598  
 1599  
 1600  
 1601  
 1602  
 1603  
 1604  
 1605  
 1606  
 1607  
 1608  
 1609  
 1610  
 1611  
 1612  
 1613  
 1614  
 1615  
 1616  
 1617  
 1618  
 1619  
 1620  
 1621  
 1622  
 1623  
 1624  
 1625  
 1626  
 1627  
 1628  
 1629  
 1630  
 1631  
 1632  
 1633  
 1634  
 1635  
 1636  
 1637  
 1638  
 1639  
 1640  
 1641  
 1642  
 1643  
 1644  
 1645  
 1646  
 1647  
 1648  
 1649  
 1650  
 1651  
 1652  
 1653  
 1654  
 1655  
 1656  
 1657  
 1658  
 1659  
 1660  
 1661  
 1662  
 1663  
 1664  
 1665  
 1666  
 1667  
 1668  
 1669  
 1670  
 1671  
 1672  
 1673  
 1674  
 1675  
 1676  
 1677  
 1678  
 1679  
 1680  
 1681  
 1682  
 1683  
 1684  
 1685  
 1686  
 1687  
 1688  
 1689  
 1690  
 1691  
 1692  
 1693  
 1694  
 1695  
 1696  
 1697  
 1698  
 1699  
 1700  
 1701  
 1702  
 1703  
 1704  
 1705  
 1706  
 1707  
 1708  
 1709  
 1710  
 1711  
 1712  
 1713  
 1714  
 1715  
 1716  
 1717  
 1718  
 1719  
 1720  
 1721  
 1722  
 1723  
 1724  
 1725  
 1726  
 1727  
 1728  
 1729  
 1730  
 1731  
 1732  
 1733  
 1734  
 1735  
 1736  
 1737  
 1738  
 1739  
 1740  
 1741  
 1742  
 1743  
 1744  
 1745  
 1746  
 1747  
 1748  
 1749  
 1750  
 1751  
 1752  
 1753  
 1754  
 1755  
 1756  
 1757  
 1758  
 1759  
 1760  
 1761  
 1762  
 1763  
 1764  
 1765  
 1766  
 1767  
 1768  
 1769  
 1770  
 1771  
 1772  
 1773  
 1774  
 1775  
 1776  
 1777  
 1778  
 1779  
 1780  
 1781  
 1782  
 1783  
 1784  
 1785  
 1786  
 1787  
 1788  
 1789  
 1790  
 1791  
 1792  
 1793  
 1794  
 1795  
 1796  
 1797  
 1798  
 1799  
 1800  
 1801  
 1802  
 1803  
 1804  
 1805  
 1806  
 1807  
 1808  
 1809  
 1810  
 1811  
 1812  
 1813  
 1814  
 1815  
 1816  
 1817  
 1818  
 1819  
 1820  
 1821  
 1822  
 1823  
 1824  
 1825  
 1826  
 1827  
 1828  
 1829  
 1830  
 1831  
 1832  
 1833  
 1834  
 1835  
 1836  
 1837  
 1838  
 1839  
 1840  
 1841  
 1842  
 1843  
 1844  
 1845  
 1846  
 1847  
 1848  
 1849  
 1850  
 1851  
 1852  
 1853  
 1854  
 1855  
 1856  
 1857  
 1858  
 1859  
 1860  
 1861  
 1862  
 1863  
 1864  
 1865  
 1866  
 1867  
 1868  
 1869  
 1870  
 1871  
 1872  
 1873  
 1874  
 1875  
 1876  
 1877  
 1878  
 1879  
 1880  
 1881  
 1882  
 1883  
 1884  
 1885  
 1886  
 1887  
 1888  
 1889  
 1890  
 1891  
 1892  
 1893  
 1894  
 1895  
 1896  
 1897  
 1898  
 1899  
 1900  
 1901  
 1902  
 1903  
 1904  
 1905  
 1906  
 1907  
 1908  
 1909  
 1910  
 1911  
 1912  
 1913  
 1914  
 1915  
 1916  
 1917  
 1918  
 1919  
 1920  
 1921  
 1922  
 1923  
 1924  
 1925  
 1926  
 1927  
 1928  
 1929  
 1930  
 1931  
 1932  
 1933  
 1934  
 1935  
 1936  
 1937  
 1938  
 1939  
 1940  
 1941  
 1942  
 1943  
 1944  
 1945  
 1946  
 1947  
 1948  
 1949  
 1950  
 1951  
 1952  
 1953  
 1954  
 1955  
 1956  
 1957  
 1958  
 1959  
 1960  
 1961  
 1962  
 1963  
 1964  
 1965  
 1966  
 1967  
 1968  
 1969  
 1970  
 1971  
 1972  
 1973  
 1974  
 1975  
 1976  
 1977  
 1978  
 1979  
 1980  
 1981  
 1982  
 1983  
 1984  
 1985  
 1986  
 1987  
 1988  
 1989  
 1990  
 1991  
 1992  
 1993  
 1994  
 1995  
 1996  
 1997  
 1998  
 1999  
 2000  
 2001  
 2002  
 2003  
 2004  
 2005  
 2006  
 2007  
 2008  
 2009  
 2010  
 2011  
 2012  
 2013  
 2014  
 2015  
 2016  
 2017  
 2018  
 2019  
 2020  
 2021  
 2022  
 2023  
 2024  
 2025  
 2026  
 2027  
 2028  
 2029  
 2030  
 2031  
 2032  
 2033  
 2034  
 2035  
 2036  
 2037  
 2038  
 2039  
 2040  
 2041  
 2042  
 2043  
 2044  
 2045  
 2046  
 2047  
 2048  
 2049  
 2050  
 2051  
 2052  
 2053  
 2054  
 2055  
 2056  
 2057  
 2058  
 2059  
 2060  
 2061  
 2062  
 2063  
 2064  
 2065  
 2066  
 2067  
 2068  
 2069  
 2070  
 2071  
 2072  
 2073  
 2074  
 2075  
 2076  
 2077  
 2078  
 2079  
 2080  
 2081  
 2082  
 2083  
 2084  
 2085  
 2086  
 2087  
 2088  
 2089  
 2090  
 2091  
 2092  
 2093  
 2094  
 2095  
 2096  
 2097  
 2098  
 2099  
 2100  
 2101  
 2102  
 2103  
 2104  
 2105  
 2106  
 2107  
 2108  
 2109  
 2110  
 2111  
 2112  
 2113  
 2114  
 2115  
 2116  
 2117  
 2118  
 2119  
 2120  
 2121  
 2122  
 2123  
 2124  
 2125  
 2126  
 2127  
 2128  
 2129  
 2130  
 2131  
 2132  
 2133  
 2134  
 2135  
 2136  
 2137  
 2138  
 2139  
 2140  
 2141  
 2142  
 2143  
 2144  
 2145  
 2146  
 2147  
 2148  
 2149  
 2150  
 2151  
 2152  
 2153  
 2154  
 2155  
 2156  
 2157  
 2158  
 2159  
 2160  
 2161  
 2162  
 2163  
 2164  
 2165  
 2166  
 2167  
 2168  
 2169  
 2170  
 2171  
 2172  
 2173  
 2174  
 2175  
 2176  
 2177  
 2178  
 2179  
 2180  
 2181  
 2182  
 2183  
 2184  
 2185  
 2186  
 2187  
 2188  
 2189  
 2190  
 2191  
 2192  
 2193  
 2194  
 2195  
 2196  
 2197  
 2198  
 2199  
 2200  
 2201  
 2202  
 2203  
 2204  
 2205  
 2206  
 2207  
 2208  
 2209  
 2210  
 2211  
 2212  
 2213  
 2214  
 2215  
 2216  
 2217  
 2218  
 2219  
 2220  
 2221  
 2222  
 2223  
 2224  
 2225  
 2226  
 2227  
 2228  
 2229  
 2230  
 2231  
 2232  
 2233  
 2234  
 2235  
 2236  
 2237  
 2238  
 2239  
 2240  
 2241  
 2242  
 2243  
 2244  
 2245  
 2246  
 2247  
 2248

864 Table 6: Comparison between speculative decoding and A3 on generating perplexity and time.  
865

	log(perplexity)	Time
Speculative decoding	<b>1.9</b>	1.2×
A3	2.1	<b>1×</b>

871 **thogonal** to speculative/MTP: these accelerations can also be applied on top of A3’s factorization in  
872 principle.  
873

874 **Comparison with recent any-subset AR.** A recent any-subset AR work ASSD (Guo & Ermon,  
875 2025) starts to provide provable joint-distribution correct parallel sampling by speculative decod-  
876 ing, which is not used in our A3 decoding process. The motivation for ASSD using correct-by-  
877 construction decoding is that, they model the sequence one token by one token using absorbing state  
878 DTMC and assume

$$879 \sum_{i \in [m, N]} \log p(x_{\sigma(i)} | \mathbf{x}_{\sigma(<m)}) \neq \log p(\mathbf{x}_{\sigma(\geq m)} | \mathbf{x}_{\sigma(<m)}). \quad (16)$$

$$880$$

881 Therefore, when they sample a new group  $\sigma(m), \dots, \sigma(N-1)$ , they need to use rejection sampling  
882 to get the right distribution for the new group. However, A3 directly models the sequence group by  
883 group. Therefore, the sampling results from  $P(x_{G_t} | x_{\cup_{j < t} G_j})$  in each step faithfully represent the  
884 true distribution.

885 We compare A3’s dynamical resampling with confidence and ASSD sampling method in uncondi-  
886 tional generation as the same setting in Figure 3 using a group size of 4. We show the results in Table  
887 7. With comparative results on generation quality, ASSD costs  $2.4 \times$  time due to additional compu-  
888 tation for resampling. This proves the high quality and high efficiency of A3’s dynamic resampling  
889 method.

890 **Practical speed-quality trade-off comparison.** We now explicitly measure decoding time for  
891 Llama-3.1-8B (AR baseline) and DiffuLlama (Diffusion baseline) under the same setting in Figure  
892 3. We evaluate all models’ log-perplexity with Llama-3.1-70B. The results are shown in Table 8.  
893 Compared with the AR baseline, with small groups (size 1 & 2), A3 achieves better performance  
894 at the trade of longer time due to more complex architecture. With moderate groups (size 4), A3  
895 achieves faster decoding than the AR baseline (67s  $\rightarrow$  37s) at a small quality tradeoff. Comapred  
896 with diffusion baseline, A3 consistently performs better with the same group size or with the same  
897 time (e.g. A3 2.1 37s v.s. DiffuLlama 2.2 51s). These results prove A3’s practical decoding effi-  
898 ciency.

899 **Results on longer contexts.** To evaluate whether A3 remains stable under significantly longer con-  
900 texts than 2k tokens, we finetuned both Llama-3.1-8B and A3-8B on 8k-length sequences from  
901 PG19 (Rae et al., 2019) using the same training budget (100 steps, batch size 64). We then eval-  
902 uated them on the single-document QA task from LongBench v1 (Bai et al., 2023b), which requires  
903 reasoning over long passages. We used dynamic sampling for A3 with group size 1 and group size  
904 2. The results are shown in Table 9.

905 A3 (group size 1) improves over the AR baseline with 1.7%, suggesting that the A3 factorization  
906 does not degrade long-context modeling and may offer small gains without parallel decoding. A3  
907 (group size 2) achieves 30% faster decoding, demonstrating that A3’s groupwise inference can  
908 provide real latency benefits in longer contexts. This result shows that larger groups introduce  
909 more parallelism but can slightly reduce accuracy, which is consistent with our analyses in shorter  
910 contexts.

911 Our 8k experiments indicate that A3 can scale to significantly longer sequences without degradation  
912 and provides decoding-time advantages via groupwise generation. These results support the poten-  
913 tial of A3 for future long-context extensions and we will explore longer context in future works.  
914

915  
916  
917

918  
919  
920  
921  
922923 Table 7: Comparison between A3’s dynamical resampling and ASSD sampling method.  
924

	log(perplexity)	Time
ASSD	2.3	2.4 $\times$
A3	<b>2.2</b>	<b>1<math>\times</math></b>

925  
926  
927  
928  
929  
930  
931  
932  
933  
934  
935  
936  
937  
938939 Table 8: Comparison with Llama-3.1-8B and DiffuLlama on speed-quality tradeoff.  
940

	log(perplexity)	Time
Llama-3.1-8B (baseline)	1.9	67s
DiffuLlama (group size = 1)	1.9	102s
DiffuLlama (group size = 2)	2.2	51s
DiffuLlama (group size = 4)	2.3	<b>25s</b>
A3 (group size = 1)	<b>1.7</b>	142s
A3 (group size = 2)	1.8	71s
A3 (group size = 4)	2.1	37s

950  
951  
952  
953  
954  
955  
956  
957  
958  
959960 Table 9: Accuracy and time comparison on Single Document QA task of LongBench v1 (Bai et al.,  
961 2023b).  
962

	QA task acc (%)	Average Time
Llama-3.1-8B (baseline)	25.4	1.0 $\times$
A3 (group size = 1)	<b>27.1</b>	1.3 $\times$
A3 (group size = 2)	22.5	<b>0.7<math>\times</math></b>

963  
964  
965  
966  
967  
968  
969  
970  
971